HAZARDOUS TOXIC ELEMENTS MOBILITY IN BURNED OIL SHALE ASH, AND ATTEMPTS TO ATTAIN SHORT- AND LONG-TERM SOLIDIFICATION

TAYEL EL-HASAN[(a)*], NIZAR ABU-JABER[(b)], NAFETH ABDELHADI[(c)]

[(a)] Faculty of Science, Mutah University, 61710, Mutah – Al-Karak – Jordan
[(b)] Department of Civil and Environmental Engineering, German Jordanian University, Naour – Amman – Jordan
[(c)] Faculty of Engineering and Technology, Al-Balqa Applied University, Amman – Jordan

Abstract. Jordan has huge organic-rich oil shale resources. The exploitation of this resource for generating electrical power by direct combustion is eminent. This process will produce huge ash tailings that contain high concentrations of potentially leachable toxic elements (e.g. Cr^{+6}, V^{+5}, As^{+3}, Cd^{+2}). This ash is friable and eventually will interact with rainwater, forming a leachate rich in toxic elements that might reach soil, plants and surface and groundwater resources. Therefore, as a preventive measure, the current study analyzed the mobility of toxic elements in the ash of burned oil shale (BOS), in particular Cr^{+6}, and aimed to fix them through mixing with other natural locally available materials such as phosphogypsum (PG) and red soil (RS). In addition, a study of the changes in mineralogy, petrography and engineering properties with time during a period of up to 12 months was conducted. The ageing results revealed that the ash + RS mixtures showed a lower leachability of toxic elements in the pH range of 5–9 in comparison with other mixtures. Besides, the said mixtures exhibited an increase in the values of unconfined compressive strength (UCS) and decrease in those of permeability (PE) unlike other mixtures. Moreover, ettringite and portlandite phases increasingly appeared in these mixtures with time, which explains the increase of UCS. The USC of the ash alone mixture was the second lowest and that of the ash + PG mixture the lowest. Therefore, mixing the produced ash with RS (3:1 ratio) under water saturation conditions would afford the best long-term solidification of harmful toxic elements.

Keywords: oil shale ash, aerobic combustion, leaching, solidification, toxic elements, ageing.

* Corresponding author: e-mail *tayel@mutah.edu.jo*

1. Introduction

Jordan has very large kerogenous limestone deposits that are often mis-characterized as being oil shales which are highly enriched in organic matter. Herein we will term them "oil shale" to conform with abundant literature data on these deposits. They are distributed in the northern, central and southern parts of the country [1]. A previous work showed the total organic carbon (TOC) of Jordan oil shale to be high, ranging from 17.39 to 22% [2]. It has been considered that such high organic matter content is suitable for enrichment of trace elements like Cr, Ni, Mo, V and the platinum group of elements (PGE) [3]. Such enrichment has been noted in Jordanian oil shales as well [4]. Alego and Maynard [5] found that trace elements were commonly considerably enriched in organic-rich facies. Recently, Jordan Oil Shale Energy Company signed a concession agreement with the Government of Jordan for the surface mining and exploitation of oil shale. There will be established an oil shale-fired power plant with a capacity of up to 900 MW. Therefore, huge ash tailings will be produced. These will very possibly contain high concentrations of leachable toxic elements [6, 7].

Because of the friable nature of the tailings, interaction of ash with rainwater might form metal-rich leachates. A study conducted in India was related to fly ash wastes generated from coal thermal plants, and explored also toxic element leachates [8].

In such cases, leachates might reach nearby soil, plants and groundwater bodies, causing hazardous pollution with toxic elements and heavy metals. As the oil shale ash is enriched in trace elements, the current study will include a retrospective monitoring of toxic elements fate. It is crucial to analyze these wastes for their content of leachable toxic metals in order to take necessary precautionary measures. This work involves investigating the mobility of toxic elements in burned oil shale (BOS) wastes, in particular of chromium, which turns out to consist mainly of toxic chromate species (Cr^{+6}), based on a previous study [9]. The extensive secondary mineral formation dynamics renders any short-term leaching tests (e.g., DIN 19529) with the highly reactive BOS of low caloric heat value. The stabilities of these phase formations under changing environmental conditions can determine the long-term mobility of toxic elements. Our approach is to verify or falsify all yet available hypotheses on possible Cr, As, V and Cd host minerals and their stabilities, as well as to test the engineering properties for solidified products.

For this purpose, a mixture of BOS ash and abundant local materials in Jordan was prepared in order to examine its long-term ageing behavior as well as the leaching characteristics of heavy metal and trace elements through time. The materials used with BOS ash included common red Mediterranean Terra Rossa soil. This type of soil would currently be classified as a vertisol on the world reference base for soil resources, and is prevalent in northwestern Jordan in areas receiving over 350 mm of precipitation per year

[10]. The clay mineral components of this type of soil are smectite/vermiculite, kaolinite, illite and palygoskite [11].

A second material tested was phosphogypsum (PG), which is an industrial by-product of the conversion of phosphate ore to phosphoric acid by reacting it with sulfuric acid. The industrial complex in Aqaba was established for this purpose, and massive amounts of PG are available. Previous investigations have shown that trace metals contained in this PG were relatively immobile, and that there were low rates of transfer between PG and the surrounding soil or water [12, 13]. Liu at al. [14] used PG as a binder in eco-friendly building products as it increased their strength. In the current work, the main expected outcomes are the scientifically-based recommendations for the best storage and recycling options for BOS ash without impacting on the surface and groundwater, soils and eco-systems.

In May 2010, Jordan Oil Shale Energy Company with a subsidiary of the Estonian company Eesti Energia signed a concession agreement with the Government of Jordan for the surface mining and retorting of oil shale. Eesti Energia and its partners will also develop an oil shale-fired electrical power plant with a capacity of up to 900 MW at Attarat um Ghudrun. The power will be supplied to National Electrical Production Company (NEPCO) pursuant to a long-term power purchase agreement. This will provide Jordan with significant power generation from a domestic source of fuel for the first time. The circulating fluidized bed combustion (CFBC) technology offers the possibility of using oil shale as a power generating fuel for direct combustion at temperatures of 700–800 °C. No additional fuel is necessary due to the high caloric heat value of oil shale, 1590 Kcal/kg, as reported by Alali et al. [15], and carbon burn-out as high as 99%. A rough calculation suggests, however, that a 900 MW thermal power plant would require 6000 tons of oil shale, releasing 3300 tons of BOS ash per day (1.2 million tons per year). Utilization of oil shale may have a severe impact on the environment because it is enriched in heavy metals as revealed in a previous study of Jordania's main deposits [2]. The aerobic combustion process of oil shale was found to concentrate toxic elements in the ash [7]. Through the interaction with rainwater and groundwater, the BOS ash would form leachate that could resemble toxic mine drainage and might reach surface and groundwater resources, causing harmful pollution. Jordan is considered one of the five most water-scarce countries in the world. A sizeable oil shale industry would substantially aggravate the water supply problem in Jordan. Therefore, it is essential to investigate the mobility of toxic elements in BOS wastes, in particular of chromium, which turns out to consist mainly of toxic chromate species. Fregert and Gruvberger [16] recorded that high temperature during clinker manufacturing at 1450 °C caused converting Cr(III) into Cr(VI). Chromates are easily soluble in an alkaline pH environment [17–19]. The expected key outcomes of this partnership are scientifically based precautionary demands made independently of the oil shale industry, such as recommendations for the best storage and recycling options for the BOS ash

without impact of leachates and dust on the surface and groundwater bodies, beside soils and other eco-systems components.

This study aims to elucidate the potential environmental impact of the Cr, V, Cd and As inventory in the ashes, develop a suitable methodology for toxic elements stabilization and immobilization, determine the elemental speciation of Cr, V, Cd and As in leachates produced from fresh and aged BOS ash samples, assess accompanying environmental risks and work out measures for stabilization of BOS ash dumps. This will necessitate leachates monitoring and collection, and, eventually, treatment of ash in the long term. This would reduce the potential pollution that might have been created by ash tailings from the oil shale industry. The study also tests the solidified aged ashes for their engineering properties and possible construction applications. Eventually, the obtained results will pave the way to an efficient, safe and sustainable oil shale industry.

2. Methodology and materials

The materials used as additives to ash mixtures are red soil (RS) from the Mutah University campus area and phosphogypsum collected from the Aqaba area. We used natural materials that are available and accessible and found in significant amounts. PG was piled up as huge tailings in the Aqaba area, as a by-product from a phosphoric acid manufacturing plant. PG is considered as an environmental pollution problem because of its high concentrations of toxic elements such as U [20–23]. However, many researchers have used PG as an additive in construction materials [20, 24]. The general approach involves working out several sequential steps, which will be discussed below.

2.1. Characterization of raw materials

A complete sieve analysis following ASTM D422 was carried out to determine the grain size distribution of the sample in addition to hydrometer analysis for the fine fraction passing #200 sieve. In order to determine the characteristics of the parent soil sample, liquid limit (ASTM D423-66) and plastic limit (ASTM D424-29, 1979) were determined. The red soil samples were classified according to the Unified Soil Classification System (ASTM D-2487) and American Association of State Highway and Transportation Officials (AASHTO) standards, specific gravity was determined according to ASTM D854. The results of these tests showed RS to have an average specific gravity 2.46, bulk density 1.17 g/cm^3, clay fraction 60.5%, unconfined compressive strength (UCS) 4.6, and plastic limit 23%.

About 50 kg of PG waste was taken from different spots from the stockpiled wastes at Aqaba industrial plant. The samples were dried at laboratory temperature, crushed and sieved. Passing sieve #100 was collected for further testing. The tested samples showed very low plasticity

to non-plastic consistency. The PG waste was mixed with ash at a ratio of 1:3 by weight. Standard compacted cylindrical samples were obtained. The samples were subjected to successive wetting and drying until testing at 1, 3, 6 and 12 months to determine their UCS and permeability (PE).

The ashing procedure was done for oil shale samples from the El-Lajjun area. The same procedure of sampling and UCS and PE testings for ash was carried out for the mixtures ash + RS and ash + PG. The tests showed that the specific gravity of ash was 2.46, moisture content 0.75 and density 1.15 g/cm^3.

2.2. Ashing and mixture preparation procedure

For ashing and mixture preparation, a certain quantity of oil shale was burnt in an aerobic combustion process up to 850 °C and 1000 °C and the additives, i.e. RS and PG, were added. The oil shale samples were collected from the El-Lajjun area, western Jordan. There were prepared three mixtures: ash alone (ash), ash + red soil (ash + RS), and ash + phosphogypsum (ash + PG). The mixtures of BOS ash, RS and PG were prepared in 10-liter plastic containers at a mixing ratio of 3:1 and were further kept in saturation with water for 1-, 3-, 6- and 12-month periods. Then the mixtures were allowed to dry, and subsequent investigations of their petrography, geochemistry and mineralogy were conducted at 1-, 3-, 6- and 12-month intervals. Besides, the mixtures were tested for their engineering properties such as unconfined compressive strength and permeability.

2.3. Ageing experiment procedure

The ageing (hydration) experiments were performed with samples of mixtures aged for 1, 3, 6 and 12 months. The ash and additives at specified ratios were mixed carefully in plastic containers and water was added to saturation to all mixtures. Each mixture was prepared in four containers for 1-, 3-, 6- and 12-month periods, respectively.

2.4. Leaching test

The leaching test was carried out for all mixtures during all ageing periods in triplicate. The sample was immersed with water with acidic, neutral and alkaline pH, i.e. 5, 7 and 9, respectively. The pH was adjusted using buffer solutions. The samples were kept in a shaker overnight. Then the leachate samples were filtered and the elute solution was poured into polyethylene bottles. The samples were further analyzed using inductively coupled plasma-mass spectrometry (ICP-MS) at Jordan University of Science and Technology (JUST), as described in the Results chapter.

2.5. Analytical procedure

2.5.1. PXRD and SEM analysis of the mineralogical composition of 1-, 3-, 6- and 12-month-old mixtures

The mineralogy of the samples of 1-, 3-, 6- and 12-month-old mixtures was studied using X-ray powder diffraction (XRD/XRPD) at the Pharmaceutical Studies Center, Jordan University of Science and Technology on a Rigaku Ultima IV device; Cu-target; 40 Kv, 40 MA, scan range 5–80 degrees; 4 degrees/minute; step width 0.02 degree; with continuous mode. Moreover, the texture of mixtures was examined through standard petrographic methods. Thin sections were made at the geology laboratory at Hashemite University and examined using a Leica petrographic transmission micro-scope at the German Jordanian University. In addition, scanning electron microscopy (SEM) was conducted at the Hamdi Mango Center in the University of Jordan.

2.5.2. The petrographical investigation of 1-, 3-, 6- and 12-month-old mixtures

Thin sections from all dried mixture samples were prepared at the Department of Geology, Hashemite University, in order to conduct mineralogical and petrographical investigations under transmitted light.

The chemical analysis of representative samples of oil shale, ash and three mixtures was carried out using X-ray fluorescence (XRF). The samples were analyzed for major oxides using a Philips PW 1404 XRF system at the Department of Geology and Mineralogy, University of Jordan. Analysis was performed according to ASTM C1271-12, loss on ignition (LOI) was determined according to section 19 of ASTM C25-11. The samples were crushed and powdered, then dried at 110 °C for 2 hours. The analysis of major and trace elements was done using the Philips PW 1404, with an attached 72-position sample changer. Pressed pellets were made by mixing 5.0 g of sample powder and 2.0 g of $L_2B_4O_7$. Bulk geochemical analysis for major and trace elements was performed using XRF at the Department of Geology and Mineralogy, University of Jordan.

pH-dependent toxic element leaching tests (TCLP) were carried out with samples of mixtures aged for 1, 3, 6 and 12 months. In the leaching tests, distilled water and analytical grade buffer solutions of pH 4 and 9 were used, solutions with three different pH values (5, 7, 9) were prepared. This was done for the entire set of samples covering the various ageing periods. 50 g samples were placed in 50 ml aliquots and allowed to soak overnight. The samples were then filtered, and the leachate was analyzed. All liquid samples obtained in this work were analyzed using an iCAP Q Thermo Scientific ICP-MS at the Department of Chemical Engineering, JUST. The leachate was diluted 10 times by using 1% nitric acid of analytical grade containing three internal standards, namely Sc, Y and Yb, to correct for instrument drift. The accuracy of the analytical procedure was achieved by making triplicate

analyses for each sample. Besides, certain samples were subjected to recurrent analysis every 10 analyses to examine any shift in instrument accuracy.

The physical and engineering properties of the aged solidified BOS samples were determined. Moreover, for engineering properties measurements additional 18 standard cylindrical samples with 50 mm in length and 25 mm in diameter were taken from the abovementioned three compacted mixtures saturated with water at a similar ratio, 3:1 by weight. The samples were dried until hardening at laboratory room temperature and kept in an open dish under successive wetting and drying conditions. UCS and PE tests of the compacted samples of 1-, 3-, 6- and 12-month-old mixtures were conducted. The analyses were carried out at Geotechnical Engineering & Materials Testing Lab.

3. Results

3.1. Geochemical results

Tables 1 and 2 present the contents of major oxides and trace elements in raw materials and in 1-, 3-, 6- and 12-month-old mixtures. Calcium (Ca), silica (Si), aluminum (Al) and sulfur (S) are the major components that distinguish the three mixtures from each other. However, because of its high share in the mixtures, the chemistry of ash dominates the three mixtures. For example, the Ca content in ash + RS was significantly increased, up to 34 wt%, but was around 14 wt% in RS. Furthermore, the high sulfur content in ash caused an increase in the SO_3 content of ash + RS mixtures. This was also seen in ash + PG whose SO_3 content was decreased to 13 wt%, but was

Table 1. XRF analytical results for major oxides content in raw materials and 1-, 3-, 6- and 12-month-old mixtures, wt%

Sample\Oxide	SiO_2	Al_2O_3	Fe_2O3	TiO_2	CaO	K_2O	MgO	Na_2O	P_2O_5	SO_3
RS	47.22	9.33	7.53	0.57	14.38	1.03	2.21	0.69	0.21	0.26
Ash	27.27	4.81	2.46	0.11	38.68	0.60	0.87	0.57	4.83	3.72
PG	7.73	0.61	0.34	0.08	39.77	0.22	0.01	0.47	11.36	36.7
Ash1	27.27	6.90	2.47	0.11	38.71	0.61	0.88	0.57	4.79	3.42
Ash3	33.22	6.54	2.29	0.27	43.66	1.20	1.23	0.34	4.80	3.27
Ash6	34.14	7.14	2.32	0.29	43.57	1.14	1.31	0.31	4.88	3.70
Ash12	33.19	6.37	2.11	0.26	41.49	1.22	1.27	0.49	4.21	3.20
A+RS1	37.85	9.86	3.80	0.62	35.33	1.69	1.65	0.24	3.68	3.08
A+RS3	38.63	10.04	3.80	0.65	34.58	1.68	1.76	0.25	3.70	3.72
A+RS6	38.90	10.34	3.78	0.64	34.75	1.68	1.83	0.26	3.81	3.81
A+RS12	39.25	9.85	3.70	0.62	34.41	1.84	1.84	0.42	3.76	3.12
A+PG1	28.48	5.45	1.74	0.06	41.07	0.95	1.07	0.33	7.49	12.62
A+PG3	27.76	5.57	1.77	0.07	41.40	0.93	1.10	0.18	7.81	12.89
A+PG6	30.13	6.00	1.78	0.07	39.61	1.02	1.27	0.53	8.30	11.59
A+PG12	30.85	5.94	1.76	0.07	39.22	1.04	1.27	0.50	8.33	11.34

Table 2. XRF analytical results for trace elements content in raw materials and 1-, 3-, 6- and 12-month-old mixtures, ppm

Sample\ Element	Mo	Zr	Sr	Rb	Se	As	Zn	Cu	Ni	Co	Mn	Cr	V	Cd	Cl	F
RS	0	250	274	21	0	8	82	21	52	18	0	98	124	0	468	730
Ash	98	39	1034	1	0	19	1070	75	290	9	29	369	155	92	863	4664
PG	15		132		0	8	94	41	19	8	249	2	113	6		500
Ash1	87	28	990	1	0	19	1039	70	293	3	18	350	150	65	25	1800
Ash3	93	32	1032	0	0	19	1067	70	297	3	13	356	157	72	27	1390
Ash6	68	32	1016	0	0	20	1059	70	296	3	25	344	155	84	27	1260
Ash12	79	29	1011	0	0	17	979	64	293	3	2	331	151	63	33	2510
A+RS1	3	80	707	16	0	7	1081	88	21	1	494	320	77	6	521	2012
A+RS3	2	75	682	17	0	8	1044	87	20	1	438	304	78	12	590	2104
A+RS6	1	67	653	20	0	8	1051	82	18	1	423	293	79	15	316	2079
A+RS12	4	68	680	19	0	8	1042	89	17	1	437	323	79	9	706	2202
A+PG1	15		602		0	4	168	39	139	8	63	161	122	4		1340
A+PG3	15		498		0	5	155	30	81	8	85	159	117	3		1580
A+PG6	16		258		0	8	115	43	54	11	88	176	112	6		970
A+PG12	14		581		0	4	162	35	132	10	58	156	99	3		1156

36 wt% in PG. Therefore, these mixtures represent different composite materials that contain all cement components. Ash contains all needed cement elements (Ca, Si, Al and S), whereas ash + RS mixtures have more pozzolanic elements (Si, Al and Fe) besides plenty of Ca and higher sulfur too. Ash + PG has a similar composition but its content of sulfur is higher and those of Al and Fe lower (Table 1).

The relatively high trace element contents in ash, such as Zn, Cr, Ni, V, Mo and Cd, affected their contents in the three mixtures having ash as their main component. Therefore, all mixtures had higher toxic element contents, particularly Cr and V (Table 2). In fact, the enrichment of these elements was the reason for elucidating the best way for their solidification. However, because of the high contents of trace elements such as Zn, Cr and V, future studies should consider possibilities of their remediation.

3.2. Mineralogy and petrography results

3.2.1. Mineralogy results

Table 3 summarizes the XRD-identified mineralogical results for mixtures. Besides, with increasing ageing period the mineral assemblages and paragenetic changes were recorded in the various mixtures used.

Table 3. XRD analysis results for raw materials and 1-, 3-, 6- 12-month-old mixtures

Sample	Mineral assemblages	Remarks
Ash RS PG	Quartz, calcite, dolomite, illite, apatite Quartz, calcite, montmorillonite Gypsum, quartz, calcite	
Ash+RS1	Quartz, calcite, illite, CASH phase, ettringite	Besides calcite and quartz, illite was decreasing with time changing to clay mineral complex phase (e.g. CASH). Ettringite seemed to fade away with time. With time emergence of portlandite and ettringite over gypsum was clear with noticeable peaks of apatite.
Ash+RS3	Quartz, calcite, illite, portlandite, ettringite	
Ash+RS6	Quartz, calcite, illite, portlandite, ettringite	
Ash+RS12	Clacite, quartz, gypsum, CASH(?), minor portlandite and ettringite and apatite	
Ash+PG1	Gypsum, basanite, quartz, calcite, perhaps anhydrite	Gradual disappearance of basanite ($CaSO_4 \cdot H_2O$) and hydration to gypsum ($CaSO_4 \cdot 2H_2O$) seen with time. After 12 months, gypsum macrofibers appeared, portlandite vanished and changed into ettringite phase.
Ash+PG3	Gypsum, basanite, quartz, calcite, ettringite, portlandite	
Ash+PG6	Gypsum, quartz, calcite, ettringite, minor portlandite and apatite	
Ash+PG12	Gypsum, ettringite, calcite, quartz, apatite, portlandite	
Ash 1	Calcite, barite, quartz, Ba-Al-Co phase, apatite(?), illite(?)	Gradual appearance of ettringite and gypsum besides amonioum chromium phase + Ba-Al-silicate phase with time (portlandite). Ettringite and portlandite became more visible and stronger after one year. Ettringite is present due to sulfate found in the ash.
Ash 3	Calcite, quartz, amonioum chromium, gypsum, quartz, Ba-Cu-Li-silicate phase, ettringite, portlandite	
Ash 6	Calcite, gypsum, portlandite, magnetite, amonioum chromium, Ba-Al-silicate, ettringite	
Ash12	Calcite, quartz, portlandite, ettringite and gypsum	

3.2.2. Petrography results

For the ash alone mixture, there is no big difference in composition between the ageing periods as shown in Figure 1. In ash1, there appears the fine-grained matrix of calcite of two types – almost amorphous and fine-grained crystalline. Also, polycrystalline rounded quartz grains can be identified and dark opaque (organic) material can be seen. In ash3, there are also visible crystalline calcite grains, with a dispersed fine-grained matrix with a lower proportion of non-crystalline calcite, polycrystalline rounded quartz grains and opaque (organic) material. The texture and composition of ash6 are similar to those of the ash3 sample. Ash12 shows an increased growth of crystals and agglomeration of Ca-Si-Al-hydrate (CASH) materials or portlandite between large calcite and clay crystals as a filling texture, which is clearly illustrated in Figure 1.
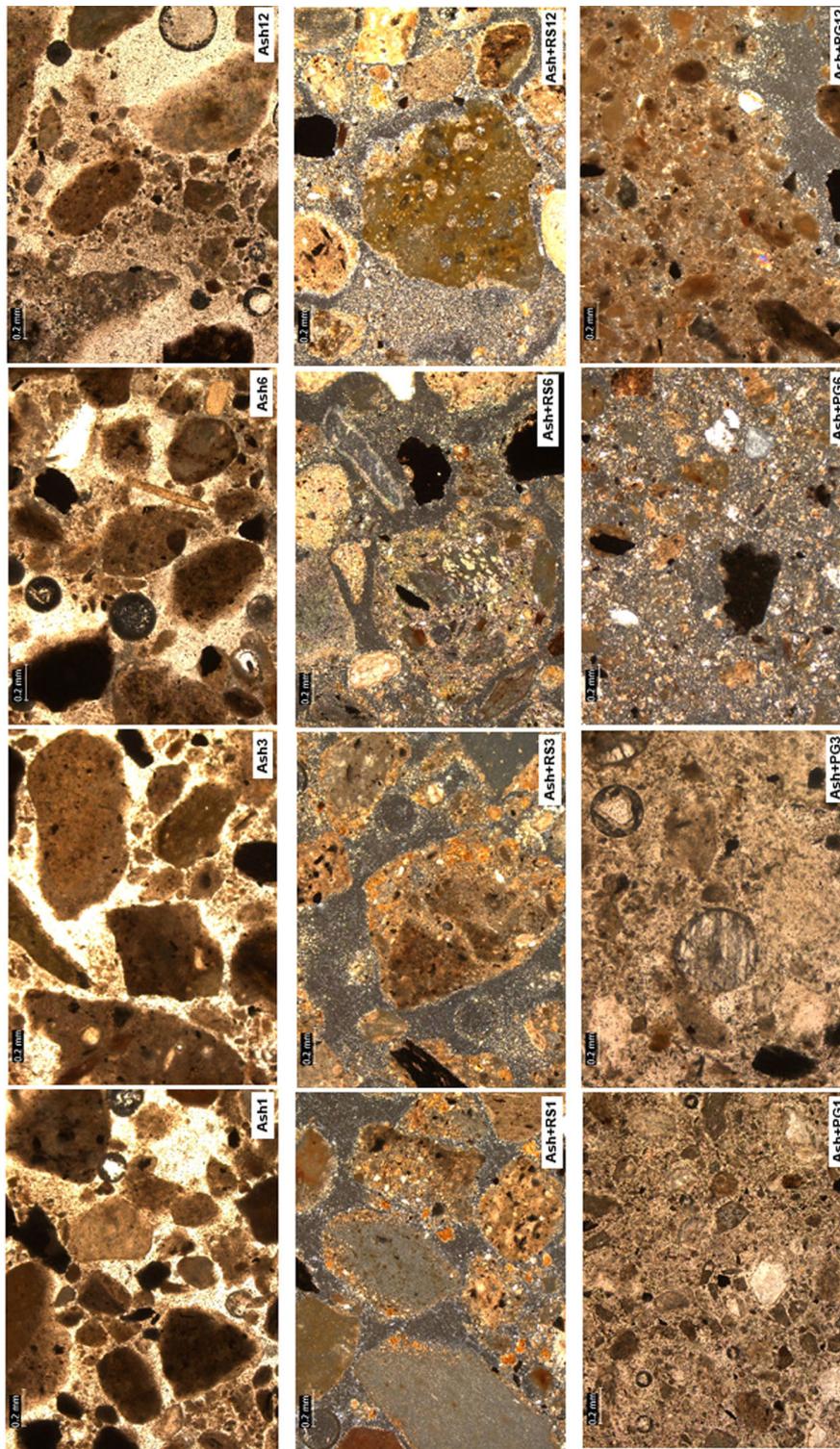
Fig. 1. Transmitted microscope photos for all mixtures and all ageing periods.

As to the ash and red soil mixtures, ash + RS1 has fine to micro-crystalline calcite with some brown grains (clay?) or agglomerations and fine-grained quartz. Opaque material (e.g. organic) was also observed. In case of ash + RS3, calcite seems to be coarser-grained here, although the crystal pattern growth looks different from that seen in the ash alone mixture, which might be attributed to the presence of pozzolanic materials that possibly encourage this different pattern of recrystallization. Also reddish globs and black opaque material are seen. In ash + RS6, the recrystallization of calcite is clearly observable within the groundmass, with some spherules of non-crystalline calcite still remaining. In ash + RS12, an obvious increase in complete filling or cementing materials are recognized as shown in Figure 1.

Regarding the ash + PG mixtures, in ash + PG1, carbonate and basanite are both fine-grained and difficult to recognize under the microscope. In ash + PG3, a tiny amount of organic material remnant can be easily seen. Recognizably, similar features can be observed in ash + PG1, but gypsum seems to begin crystallization. In ash + PG6, the crystal growth of calcite and gypsum is more obvious, besides, some CaO + Al-sulphate-hydrate (CASH) materials are visible. Black holes (possibly voids) are found within the matrix. Although there is a more significant growth of gypsum and calcite crystals in ash + PG12, new CAŜH materials (i.e. ettringite) emerge, besides, black holes are still there. These changes are illustrated in Figure 1. Similarly, Liu et al. [14] had recognized the formation of CASH and ettringite in a PG-based building binder.

3.3. Engineering properties

The results of engineering properties tests showed that the unconfined compressive strength of ash alone and ash + RS mixtures gradually increased, to 47 kg/cm^2 and 46.8 kg/cm^2, respectively, during a 12-month ageing period. At the same time, the UCS of the ash + PG mixture reached only 26 kg/cm^2 during the same span of ageing. The permeability values of ash alone and ash + RS mixtures were lower, $7.37 \cdot 10^{-6}$ and $3.95 \cdot 10^{-6}$ cm/sec, respectively, after a 12-month ageing. The PE of the ash + PG mixture was higher, up to $5.89 \cdot 10^{-5}$ cm/sec, after the same period of ageing. These results are illustrated in Figure 2.

3.4. Leaching test results

The leaching tests were conducted with all mixtures at all ageing intervals with respect to various pH values, i.e. 5, 7 and 9. There was noticed that a lower pH of the solution increased the leachability of toxic elements. However, the ash + RS mixture had the lowest values of leached toxic elements. The leaching results for selected toxic elements (Mo, Se, Cr and V) are shown in Figures 3a–c.
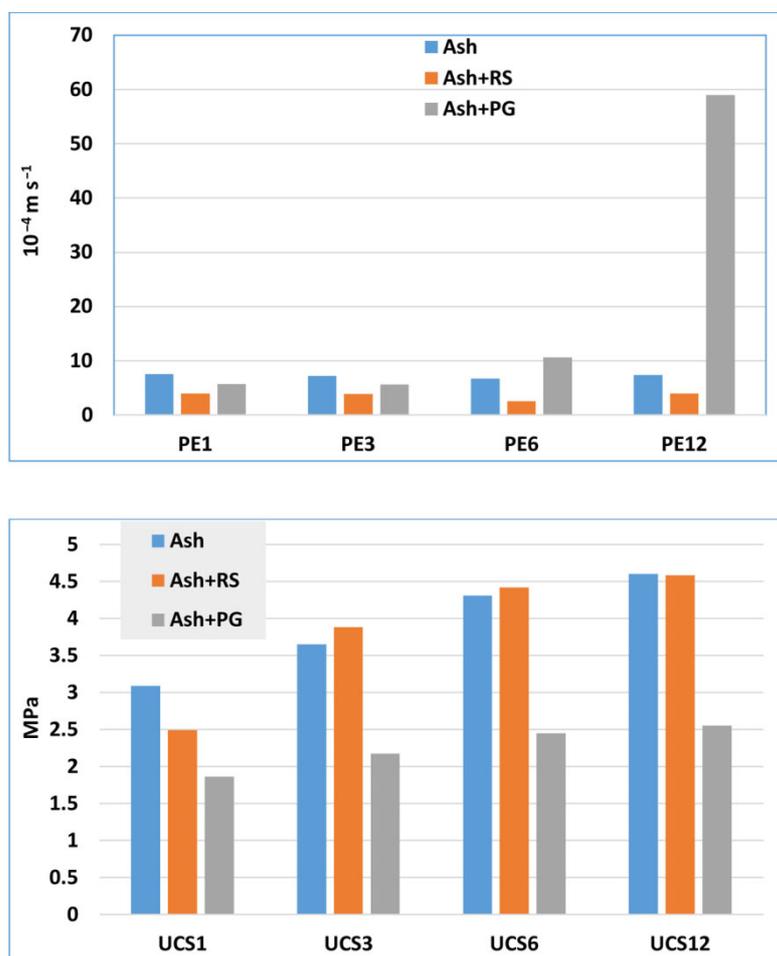
Fig. 2. Histogram illustrating changes in UCS and PE of the three mixtures of all ages.

4. Discussion

4.1. Mineralogy and petrography

The minerals in the samples represent a mixture of both primary and secondary minerals. As seen from Table 3, RS is a mixture of quartz, calcite, illite and montmorillonite. PG consists of gypsum with traces of apatite, quartz and calcite, while ash is composed of calcite, quartz, apatite and illite. In the ash alone mixture samples, secondary minerals such as portlandite $(Ca(OH)_2)$ and ettringite $(Ca_6Al_2(SO_4)_3(OH)_{12}\cdot26H_2O)$ appear. Anhydrite $(CaSO_4)$ and basanite $(CaSO_4\cdot H_2O)$ are found in the ash + PG mixture. Anhydrite reverts to gypsum with time. The XRF analysis showed silica and calcium oxides to be present in most samples and PG to contain about 10–12% SO_3 (Table 1).
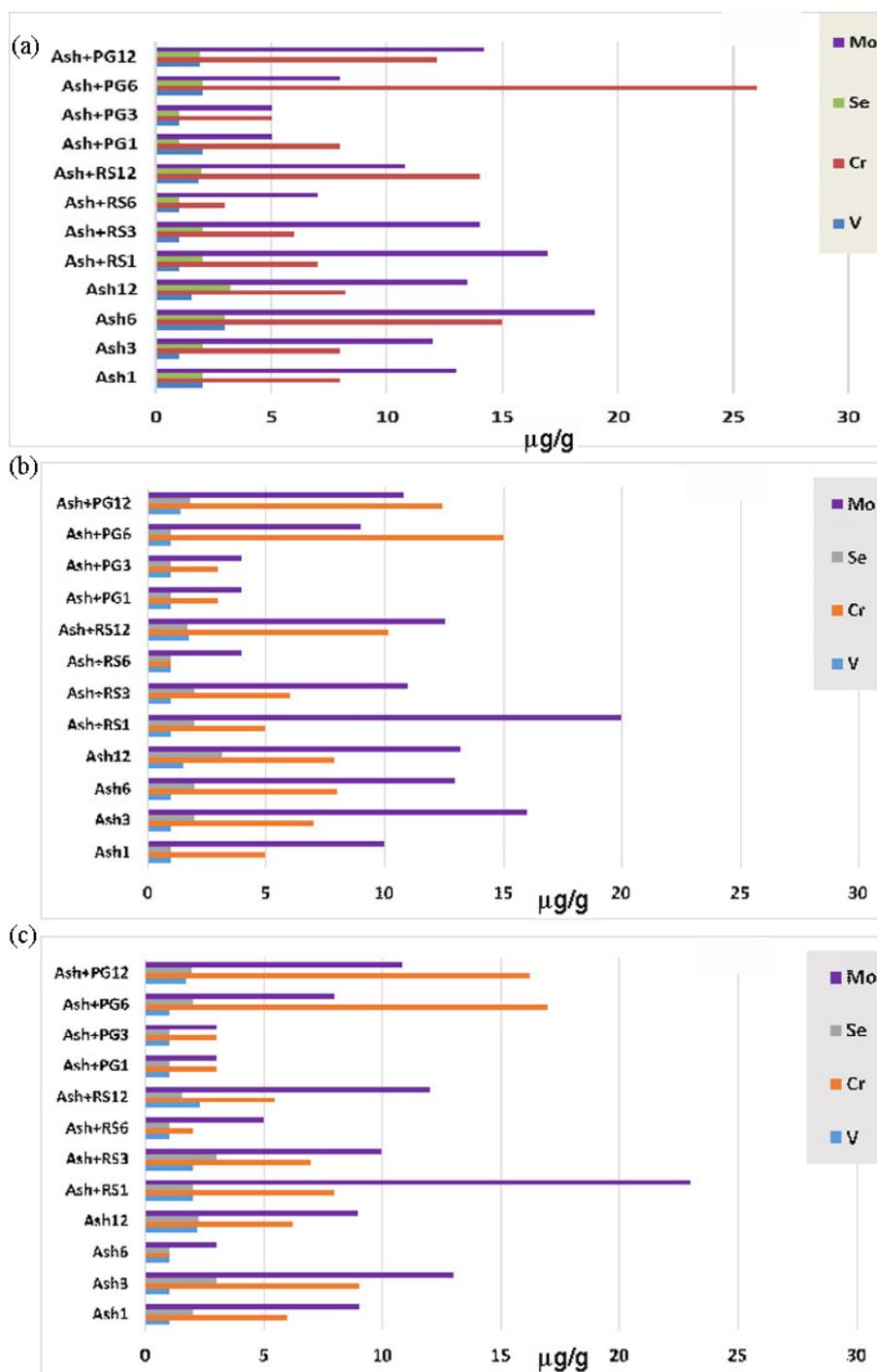
Fig. 3. Histograms showing the effect of pH of solution on the leachability of toxic elements from all studied mixtures of all ageing periods: a) pH 5; b) pH 7; c) pH 9.

As ash comes primarily from the burning of kerogen-rich limestone, it is expected that the calcite present in the rock would break down to form lime:

$$CaCO_3 + heat \longrightarrow CaO + CO_2$$

In turn, the lime takes up water from a variety of sources to form portlandite. This could be the free water used in the experiment:

$$CaO + H_2O \longrightarrow Ca(OH)_2 + 2H^+$$

In the case of the ash + PG mixture, molecular water seems to have been removed from gypsum to produce basanite:

$$CaO + CaSO_4 \cdot 2H_2O \longrightarrow Ca(OH)_2 + CaSO_4 \cdot H_2O + 2H^+$$

Ultimately, basanite takes up available moisture to revert to gypsum. These processes were observed to occur in all data sets, i.e. XRD, petrography and SEM, as shown in Figure 4.

Petrographic investigations of the ash alone mixture revealed a heterogeneous mixture of angular portlandite and fine-grained unidentifiable and opaque minerals, which is indicative of a small change through the ageing periods. This can be seen in the ash3 and ash6 samples which display the growth of abundant secondary needles. In the aged sample of ash12, new orthorhombic crystals of portlandite appeared (Fig. 5).

The ash + RS mixtures contain polymineralic phases of various grain sizes bound by undifferentiated fine-grained material which is probably clay introduced as part of the soil component of the mixture. The initial mixtures of ash + RS comprise platy agglomerations covering the surface of the fine-grained ash. These, in turn, display the overgrowth of fine secondary needles, some of which having a radial growth pattern. The ash + RS3 samples exhibit a continuous growth of secondary needles, some of which appearing on coarser-grained substrates. In the ash + RS6 samples, short tetragonal prisms begin to appear in addition to the abundant fine-grained needles, i.e. ettringite. The ash + RS12 samples exhibit the growth of secondary crust in addition to the fine-grained needles. The latter are seen in all SEM images and seem to be ettringite (Fig. 5).

Ettringite is formed as a result of combination of calcite and aluminum-containing materials with access of sulfur. This is visible in the SEM images as short prismatic crystals, which suggests that the mineral is not the direct result of the burning process as these crystals appear at a later stage. Moreover, the XRD data demonstrates that ettringite appears mostly in the ash + PG and ash + RS mixtures.

The ash + PG mixture develops a botryoidal texture, after 3 and 6 months, prismatic-fibrous crystals begin to appear within the botryoidal matrix. The ash + PG12 mixture reveals the earlier growth of the needle-like crystals of ettringite, in addition to the rare prismatic crystals of portlandite. The SEM investigation showed that ash started to form as a very fine-
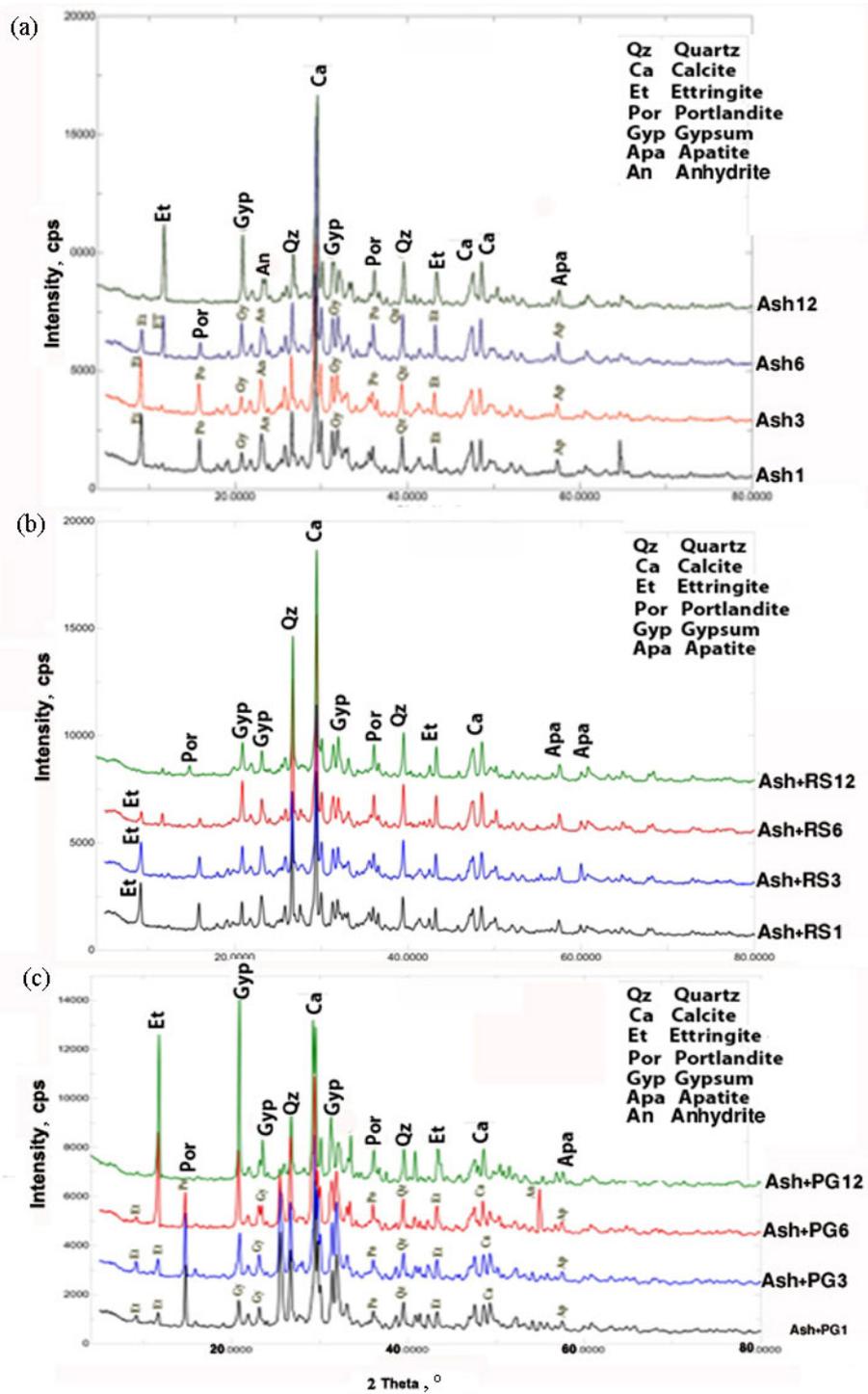
Fig. 4. Overplayed XRD charts for mixtures of all ageing periods: a) ash; b) ash + RS; c) ash + PG.
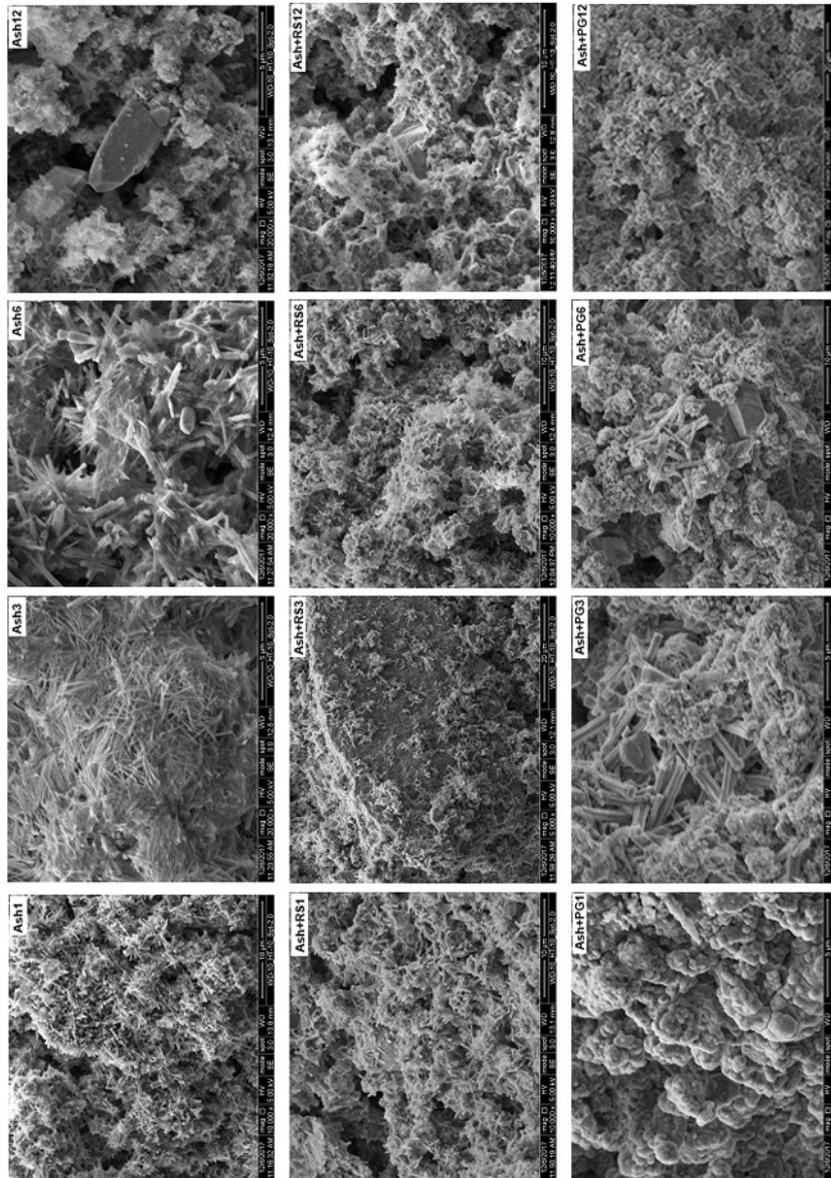
Fig. 5. SEM micrographs for the three mixtures of all ageing periods.

grained spheroidal (μm scale) homogenous material, with the modest growth of secondary needles. With ageing, the needles seemed to grow at the expense of primary spheroids (Fig. 5).

4.2. Interpretation of engineering test results

4.2.1. Unconfined compressive strength

All the tested samples were subjected to successive wetting and drying cycles during the curing time which extended from one month to one year. The testings were performed after different periods of ageing. The unconfined compressive strength of the tested ash samples had increased from 31.6 to 44 kg/cm^2 after a 6-month ageing, while the rate of UCS build-up increased a little,1 kg/cm^2, during the ageing period from 6 to 12 months as shown in Figure 2.

The hydration reactions between the alkali (CaO) and pozzolanic parts in the ash samples produced portlandite (Ca(OH)$_2$) and a fibrous calcium silicate hydrate compound (C-S-H), which was responsible for the strength build-up in the tested samples. The high UCS might be due to that ash acted as a self-cementitious material. The increase of UCS is proportional to the C-S-H content in the tested samples as seen in the scanning electron micrographs (Fig. 5).

The UCS of the ash + RS mixtures changed similarly to the ash alone mixture's, increasing from 25.4 kg/cm^2 at one month to 46.8 kg/cm^2 at six months, remaining thereafter unchanged to the end of the 12-month period. Similarly to the ash alone mixture, the abundance of CaO was the governing factor, in addition to clay that provided pozzolanic components, which resulted in an increase of UCS.

Lower UCS values were recorded in all aged ash + PG samples. The UCS was 19 kg/cm^2 at one month and rose to 25 kg/cm^2 at six months, while at 12 months it was increased by only 1 kg/cm^2 to reach 26 kg/cm^2. The SEM micrograph reveals a minor content of C-S-H and a high content of ettringite (Fig. 5). The mineral ettringite (calcium aluminum silicate sulphate) is the output of the reaction of the alkali part (CaO) and Si and Al from the ash and sulphate from phosphogypsum. Thus, the UCS of ash + RG mixtures is low compared with ash alone and ash + RS. Now the excess of sulphate would increase the growth of ettringite crystals, causing the internal tensile stress to increase, which triggers the cracking. These cracks are considered as secondary porosity features (Fig. 5). The UCS recorded in the current study is lower than that obtained by Liu et al. [14]. This might be due to the fact that the investigators used different components of the matrix, i.e. slag and cement, while the authors of the current work used only ash and PG.

4.2.2. Permeability results

To obtain permeability at the same laboratory temperature, the falling head method was used. The PE of ash samples was very low, ranging from

$7.48 \cdot 10^{-06}$ to $7.37 \cdot 10^{-06}$ cm/sec, while that of ash + RS samples varied between $3.90 \cdot 10^{-06}$ and $3.95 \cdot 10^{-06}$ cm/sec. Both mixtures had quite similar PE values, whereas the trivial variation was due to the similar grain size distribution in them. However, the PE of ash + PG increased with time as illustrated in Figure 2. This was due to the growth of ettringite crystals related to the existence of a rich sulphate environment and successive wetting and drying of the samples over the curing period which extended to one year since molding. The development of larger crystals of ettringite through its late formation led to the appearance of pores and microcavities in the mixture as revealed in the SEM graphs in Figure 5.

Ca-Si-Al-hydrate is a complex compound which is responsible for concrete strength. The pozzolanic part (silica-aluminum-Fe_2O_3) of CASH came from RS and CaO originated from ash, which explains the increase in UCS and lower permeability of the ash + RS mixture.

In case of ash + PG, the CAŜH, i.e. ettringite, would form at a place where sulphate is replacing silica. The previously mentioned abundance of sulphate caused the cracking, which might also explain the increase in PE, together with the decrease of the UCS of ash + PG, contrarily to ash alone or ash + RS mixtures. Moreover, the strength of CASH is usually higher than that of CAŜH, which explains the lower UCS of the PG-containing mixture compared to other mixtures, as shown in Figure 2.

Portlandite [$Ca(OH)_2$] is usually formed when there is an excess of CaO as in the case of the ash alone mixture. In the current work, portlandite was considered as a lime saturation factor because of the deficiency in silica and Al which led to the formation of $Ca(OH)_2$. Portlandite would slightly increase the strength of the mixture with time. If CO_2 is available from air and rainwater, it will be absorbed and react with portlandite to revert to calcite according to the following equation:

$$Ca(OH)_2 + CO_2 \longrightarrow CaCO_3 + H_2O$$

However, the ash + RS mixture can provide the best chemical assemblage (CaO + pozzolanic components) at ambient concentrations that would produce high strength and low permeability concrete. At the same time, the UCS of the ash alone mixture may be slightly lower than that of the ash + RS mixture, but would increase with time.

4.3. Interpretation of leaching test results

The majority of the elements, such as Al, Fe, Mn, Rb, Bi, U, Pb, Zn, Co, Cu, Ni As and Cd, were not detected in leaching solutions at any tested pH values. However, Ca, Mg, K and Ba were found to be present in moderate contents. Besides, very low concentrations of toxic elements such as Cr, V, Se and Mo were detected (Fig. 3).

Regarding Ca, Mg, K and Sr, generally, a solution with pH 5 afforded higher concentrations of leachates. Particularly, calcium leaching was the highest at pH 5, with similar leaching characteristics in case of all sample

mixture types and ageing times. A slightly higher leaching was observed in the ash1 and ash + PG1 mixtures. Potassium leaching was the highest at pH 5. In the case of magnesium, the leachability of the solution of pH 5 was significantly higher compared to the solutions with other pH values. In all tests, the leaching rates were similar for different mixtures with similar ageing periods. Moreover, with increasing ageing the leaching rates were increased for all sample mixtures. This gave evidence for the elemental dissolution due to continuous water saturation.

The leaching rate was similar in tests with solutions of pH 7 and 9. The lowest leaching rate was observed with the ash + RS mixture at pH 7, while the leaching rate of Ca, Mg and Sr solutions increased and that of the K solution decreased with ageing. At pH 9, the leaching of pure ash samples progressively decreased with ageing, while that of ash + PG and ash + RS mixtures increased with increasing ageing.

The concentrations of toxic elements in leaching solutions at pH 7 were the lowest, compared with solutions whose pH was 5 or 9 (Fig. 3). And, mostly the ash + RS mixture had the lowest concentrations of leached elements. In fact, the leachability of this mixture decreased with time, reaching its lowest value after 6 months (ash + RS6). However, a characteristic trend was observed with all mixtures at all pH values when the concentration of leached elements increased reversely to the previous behavior after 6 months of ageing, particularly in case of ash + RS6. This might be attributed to the effect of continuous water saturation after 6 months, which may have caused re-dissolution of elements that was accompanied with further mineralogical changes. This phenomenon has previously been observed in other researches too [25, 26]. Therefore, it seems that water saturation should be discontinued or gradually decreased until the end of a 6-month period for all mixtures in order to stop elemental re-dissolution.

The higher concentrations of leached elements were observed at pH 5, which was attributed to the acidic media favourable for the elements mobility and dissolution. Neutral pH 7 may change to slightly acidic affinity with time if in the area of mining the sulfur emissions reach the surface water or rainwater and, as a result, decrease the acidity of water, thus causing an increase in the dissolution of toxic elements contained in the ash tailings. Therefore, precautionary measures should be taken to prevent the emission of gases, particularly sulfur, and the acidification of water.

The leaching of toxic elements such as chromium was maximum from the ash + PG mixture, and was especially pronounced in the leaching test at pH 5 (Fig. 3). At the same time, the leaching of molybdenum from the ash + RS mixture was the lowest This might be related to the increase of permeability with time in all mixtures. The ash alone mixture had the highest PR in the early stages, but with time that of the ash + PG mixture increased most. The permeability of the ash + RS mixture remained low throughout the whole ageing period, and the UCS of all samples increased with time. This explains why the UCS values of ash alone and ash + RS mixtures were similar, being

at the same time higher than that of the ash + PG mixture, whose UCS was the lowest and PE higher.

Furthermore, the leaching characteristics of calcium seemed to reflect the re-carbonization of portlandite in the ash samples as low-pH (5) solutions primarily dissolve $CaCO_3$. The ash + PG mixture best retained molybdenum, although the progressive reversion to gypsum increased the leaching of this heavy metal with time. This might be related to the increase of PE and decrease in UCS, which was characteristic of the ash + PG12 mixture. A similar pattern could be seen with chromium. The leached amounts of selenium and vanadium were the lowest throughout the entire experiment and across the entire pH range. At the same time, the ash + PG mixture could lead to a short-term immobilization of toxic elements, but this advantage was lost with time.

It is interesting to note that the ash + RS mixture slightly decreased the leaching of toxic elements. This is especially notable given that the amount of heavy metal bearing ash is diluted when mixed with other components. Thus, a considerable advantage emerges from forming such mixtures to minimize toxic elements leaching. There is a clear benefit from using RS as an additive to minimize leaching under natural pH conditions. This is in agreement with the increase in UCS and decrease of PE due to mineralogical changes, i.e. the formation of CASH minerals. Furthermore, Cr(VI) in the form of $CrO4^{-2}$ was found to form a solid solution with $SO4^{-2}$ in ettringite in the cementitous system, due to the identical charges and comparable radii [17, 27–30]. The hydration process is very essential in the bonding of chromate into hydration cementitious products, lowering Cr leaching [31, 32].

The adverse effect of continuous water saturation on toxic elements leaching could be explained by the fact that ash is carbonaceous in nature and when saturated with water the pH increases, turning the environment alkaline. Some elements such as Cu, Zn, Cd and Pb are not highly mobile due to their strong surface adsorption in a highly alkaline environment [33]. However, in the same environment, Mo, As, Se and Cr(VI) are mobile [34]. Nevertheless, at a relatively low pH (< 10.7) Ca-sulfoaluminates become metastable and start to decompose into Ca-sulfate (e.g. gypsum and bassanite), Al gel and carbonate polymorph [35–37]. Therefore, the increase of pH due to continuous water saturation may be the reason for the desorption of toxic elements (Cr, Mo, V) into the leachate after a 6-month ageing. This holds true also for ash + PG whose leaching is adversely influenced by the long-term saturation, increasing the mobility of said metals. Moreover, the high sulphate content may in fact lead to the formation of complexes that increase the mobility of chromium and molybdenum when the mixture ages, and cause secondary porosity and cracking that lowers the UCS and PE of the ash + PG mixture.

5. Conclusions

1. The results of the accomplished tests demonstrated noticeable variations between the three mixtures. The ash + red soil and ash alone mixtures showed the lowest concentrations of leached toxic elements with increasing ageing, indicating them to be the most suitable additives for a better ash tailings solidification and toxic elements immobilization.
2. The results of the leaching test for all mixtures at all ageing intervals with respect to various pH values (i.e. 5, 7 and 9) showed that there was a notable trend of the effect of lower pH of solution on increasing the leachability of toxic elements. Moreover, the mixture composed of ash and red soil had the lowest leaching values of toxic elements. This was in agreement with the petrographic coagulation texture formed in a particular texture and the higher values of unconfined compressive strength and lower figures of permeability.
3. The X-ray diffraction revealed that in the mixture with red soil as an additive there appeared increasing cement mineral assemblages such as ettingrite and portlandite with ageing. This was evidenced by the higher unconfined compressive strength and lower permeability values of this mixture compared with other mixtures**.**
4. The most plausible natural pH in the real world is that of natural water. The lowering of pH values can be achieved through continuous saturation which may lead to toxic elements dissolution. This was evidenced by the increase in leaching rate after a 6-month ageing period.
5. Gas emissions from oil shale plants, particularly sulfur, could cause acidification of water resources and rainwater in the area, thus accelerating the leaching of toxic elements.
6. It is possible to achieve in ash higher concentrations of metals of economic value such as Zn, Cr, Ni and V. Therefore, further investigation should be concentrated on the means of remediation of these metals.

REFERENCES

1. Hamarneh, Y. *Oil Shale Resources in Jordan.* NRA, Amman, Jordan, 1998, 98 pp.
2. El-Hasan, T. Geochemistry of the redox-sensitive trace elements and its implication on the mode of formation of the Upper Cretaceous oil shale, Central Jordan. *Neues Jb. Miner. Abh.*, 2008, **249**(3), 333–344.

3. Coveney, R. M., Nansheng Jr, C. Ni-Mo-PGE-Au-rich ores in Chinese black shales and speculations on possible analogues in the United States. *Miner. Deposita*, 1991, **26**(2), 83–88.

4. Ibrahim, K. M., Jaber, J. O. Geochemistry and environmental impacts of retorted oil shale from Jordan. *Environ. Geol.*, 2007, **52**(5), 979–984.

5. Algeo, T. J., Maynard, J. B. Trace-element behavior and redox facies in core shales of Upper Pennsylvanian Kansas-type cyclothems. *Chem. Geol.*, 2004, **206**(3–4), 289–318.

6. Al-Ghouti, M. A., Al-Degs, Y. S., Ghrair, A., Khoury, H., Ziedan, M. Extraction and separation of vanadium and nickel from fly ash produced in heavy fuel power plants. *Chem. Eng. J.*, 2011, **173**(1), 191–197.

7. El-Hasan, T. Characteristics and environmental risks of the oil shale ashes produced by aerobic combustion and anaerobic pyrolysis processes. *Oil Shale*, 2018, **35**(1), 70–83.

8. Kapoor, S., Christian, R. A. Transport of toxic elements through leaching in and around ash disposal sites. *International Journal of Environmental Science and Development*, 2016, **7**(1), 65–68.

9. El-Hasan, T., Szczerba, W., Buzanich, G., Radtke, M., Riesemeier, H., Kersten, M. Cr(VI)/Cr(III) and As(V)/As(III) ratio assessments in Jordanian spent oil shale produced by aerobic combustion and anaerobic pyrolysis. *Environ. Sci. Technol.*, 2011, **45**(22), 9799–9805.

10. Lucke, B. *Landscape Transformations in the Context of Soil Development, Land Use, and Climate. A Comparison of Marginal Areas in Jordan, Mexico, and Germany.* Borntraeger Science Publishers, Stuttgart, Germany, 2017.

11. Khresat, S., Taimeh, A. Properties and characterization of vertisols developed on limestone in a semi-arid environment. *J. Arid Environ.*, 1998, **40**(3), 235–244.

12. Hou, C., Huo, D. Performance and application of phosphogypsum. *Chemistry Industry and Mine Technology*, 1997, **26**(2), 50–52 (in Chinese).

13. Al-Hwaiti, M. S., Ranville, J. F., Ross, P. E. Bioavailability and mobility of trace metals in phosphogypsum from Aqaba and Eshidiya, Jordan. *Geochemistry*, 2010, **70**(3), 283–291.

14. Liu, L., Zhang, Y., Tan, K. Cementitious binder of phosphogypsum and other materials. *Adv. Cem. Res.*, 2015, **27**(10), 567–570.

15. Alali, J., Abu Salah, A., Yasin, S., Al Omari, W. *Mineral Status and Future Opportunity: OIL SHALE.* Ministry of Energy and Mineral Resources, Unpublished report, 2015, 26.

16. Fregert, S., Gruvberger, B. Factors decreasing the content of water-soluble chromate in cement. *Acta Derm-Venerol,*, 1973, **53**(4), 267–270.

17. Leisinger, S. M., Lothenbach, B., Le Saout, G., Kägi, R., Wehrli, B., Johnson, C. A. Solid solutions between CrO_4- and SO_4-ettringite $Ca_6(Al(OH)_6)_2[(CrO_4)_x(SO_4)_{1-x}]_3 \cdot 26\,H_2O$. *Environ. Sci. Technol.*, 2010, **44**(23), 8983–8988.

18. Zhang, M. *Incorporation of Oxyanionic B, Cr, Mo and Se into Hydrocalumite and Ettringite: Application to Cementitious Systems*. Ph.D. Dissertation, University of Waterloo, Ontario, Canada, 2000.

19. Palmer, C. D. Precipitates in a Cr(VI)-contaminated concrete. *Environ. Sci. Technol.*, 2000, **34**(19), 4185–4192.

20. Abdelhadi, N., Abdelhadi, M., El-Hasan, T. The characteristics of cement mortars utilizes the untreated phosphogypsum wastes generated from fertilizer

plant, Aqaba-Jordan. *Jordan Journal of Earth and Environmental Sciences (JJEES)*, 2014, **6**(2), 61–66.

21. Abdelhadi, M., Abdelhadi, N., El-Hasan, T. Optimization of phosphogypsum by-production using orthophosphoric acid as leaching solvent with different temperatures and leaching time periods. *Earth Science Research*, 2018, **7**(2), 28–41.

22. Rabba, I. A. M. M. Geochemistry, mineralogy and petrography of Al-Hisa phosphate rocks and its upgraded ores. *Journal of Environment and Earth Science*, 2016, **6**(2), 26–33.

23. Al-Hwaiti, M. S., Brumsack, H. J., Schnetger, B. Suitability assessment of phosphate mine waste water for agricultural irrigation: an example from Eshidiya Mines, South Jordan. *Environmental Earth Sciences*, 2016, **75**(3), Article 276.

24. Mymrin, V. A., Alekseev, K. P., Nagalli, A., Catai, R. E., Romano, C. A. Hazardous phosphor-gypsum chemical waste as a principal component in environmentally friendly construction materials, *J. Environ. Chem. Eng.*, 2015, **3**(4, Part A), 2611–2618.

25. Dames, A., Moore, R. *Environmental Baseline Studies, Red Dog Project. Water Quality Report*, Chapter 3, prepared by L. A. Peterson and Associates, Inc., for the Red Dog Mine Project, Cominco, Alaska, Inc., Anchorage, Alaska, 1983.

26. USBLM (United States. Bureau of Land Management). Rio Puerco Resource Area. *Rio Puerco Resource Management Draft Plan & Environmental Impact Statement*. Bureau of Land Management, Albuquerque District, Rio Puerco Field Office, 2012, 327.

27. Wang, S., Vipulanandan, C. Solidification/stabilization of Cr(VI) with cement: Leachability and XRD analyses. *Cement Concrete Res.*, 2000, **30**(3), 385–389.

28. Evans, N. D. M. Binding mechanisms of radionuclides to cement. *Cement Concrete Res.*, 2008, **38**(4), 543–553.

29. Moulin, I., Rose, J., Stone, W., Bottero, J.-Y., Mosnier, F., Haehnel, C. Lead, zinc and chromium (III) and (VI) speciation in hydrated cement phases. In: *Waste Management Series* (Woolley, G. R., Goumans, J. J. J. M., Wainwright, P. J., eds.). Elsevier, New York, 2000, 269–280.

30. *Chromium* (Langard, S., Costa, M., eds.). Academic Press, Inc., New York, 2007.

31. Van der Sloot, H. A. Comparison of the characteristic leaching behavior of cements using standard (EN 196-1) cement mortar and an assessment of their long-term environmental behavior in construction products during service life and recycling. *Cement Concrete Res.*, 2000, **30**(7), 1079–1096.

32. Park, J.-Y., Kang, W.-H., Hwang, I. Hexavalent chromium uptake and release in cement pastes. *Environ. Eng. Sci.*, 2006, **23**(1), 133–140.

33. Adamson, J., Irha, N., Adamson, K., Steinnes, E., Kirso, U. Effect of oil shale ash application on leaching behaviour of arable soils: An experimental study. *Oil Shale*, 2010, **27**(3), 250–257.

34. Cornelis, G., Johnson, C. A., Van Gerven, T., Vandecasteele, C. Leaching mechanisms of oxyanionic metalloid and metal species in alkaline solid wastes: A review. *Appl. Geochem.*, 2008, **23**(5), 955–976.

35. Nishikawa, T., Suzuki, K., Ito, S., Sato, K., Takebe, T. Decomposition of synthesized ettringite by carbonation. *Cement Concrete Res.*, 1992, **22**(1), 6–14.

36. Myneni, S. C. B., Traina, S. J., Logan, T. J. Ettringite solubility and geochemistry of the $Ca(OH)_2$–$Al_2(SO_4)_3$–H_2O system at 1 atm pressure and 298 K. *Chem. Geol.*, 1998, **148**(1–2), 1–19.
37. Liira, M., Kirsimäe, K., Kuusik, R., Mõtlep, R. Transformation of calcareous oil-shale circulating fluidized-bed combustion boiler ashes under wet conditions. *Fuel*, 2009, **88**(4), 712–718.